RSC Advances

The Absorption of Water-soluble Ionic Liquids on Graphene Oxide of Different Oxygen Content

SCHOLARONE™
Manuscripts

1   **The Adsorption of Water-soluble Ionic Liquids on Graphene**

2   **Oxide of Different Oxygen Content**

3   Tian Longlong[1] and Zhang Xin[2], Qi Wei[1], Liu Dan[1], Jin Qiang[1], Lin Jing[1], Ye

4   Yuanlv[4], Li Zhan[3*], Wu Wangsuo[1*]

5   1. Radiochemical Laboratory, Lanzhou University, Lanzhou, Gansu, China, 730000

6   2. Institute of Modern Physics, Chinese Academy of Sciences, Lanzhou, Gansu, China,

7   730000

8   3. Lanzhou Institute of Chemistry Physics, Chinese Academic of Science，Lanzhou,

9   Gansu, China, 730000

10   4. Nuclear and Radiation Safety Center, Ministry of Environmental Protection of

11   China, Beijing, China, 100082

12   Corresponding author: Li Zhan, Email: lizhancg@licp.cas.cn; Wu Wangsuo, Email:

13   wuws@lzu.edu.zn.

14   **Abstract**: With the large-scale study and application of graphene and ionic

15   liquids (ILs), it was imperative to clarify their interaction mechanism in environment.

16   The graphene oxides (GO) with different oxygen content were obtained using electron

17   beam irradiation and chemical reduction. Then batch adsorption experiments were

18   preformed to understand the adsorption behavior of ILs on GO with different oxygen

19   content. Experiment results show that adsorption capacity of ILs on GO depend

20   strongly on the oxygen level of graphene and ionic strength of solution, GO of rich

21   and poor oxygen presented better performances at high and low ionic strength,

22   respectively, which is owing to the formation of chemical bonds between ILs and

1   oxygen groups on GO. Moreover, ILs own the dual properties of aromaticity and

2   cation in favor of the adsorption of ILs on GO. Competitive adsorption of two ILs on

3   GO of poor oxygen content was observed; but one IL could promote the adsorption of

4   the other ILs on GO of rich oxygen content, these could be attributed to the properties

5   of ILs and GO. This work might advance the understanding of the adsorption

6   behavior of ILs on graphene oxide and find a possible way to remove ILs in the

7   environmental systems.

8   **Keyword**: Graphene oxide; Different oxygen content; Room temperature

9   ionic liquid; Adsorption behavior;

10   **Introduction**

11   Room temperature ionic liquids (ILs) are made of positively and negatively

12   charged ions[1], have favorable properties as green solvents and catalysts for chemical

13   reactions and processing[2] and have come into practical use in industry[3-7]. Since their

14   releasing to the environment is inevitable, environmental fate and toxicity of ILs have

15   become important topic[8]. Some papers reported that ILs exhibit toxicities[9] on

16   organisms, bacteria, algae, duckweed, daphnia, and zebrafish. The sorption behavior

17   of ILs in environmental systems such as natural soils, aquatic sediments, and bacterial

18   and mineral surfaces shows that the migration of ILs readily occurs, especially for

19   water-soluble ILs, leading to a potential hazard for life and ecosystem[10]. Thus, their

20   controlled removal or recovery by oxidation, biodegradation, and adsorption, from all

21   possible sources, especially water, have been considered, to avoid their long-term

22   adverse consequence to the environment[11]. In addition, a variety of ILs will be

1   discharged inevitably into the water in environment together in application of industry,

2   so it is necessary and important to research combined adsorption of two or multiple

3   ILs for solving real pollution problem.

4   Carbon nanomaterials have been widely studied in the last decades[12-17].

5   Graphene, a single atomic layer of *sp²* carbon atoms two-dimension material, is

6   promising materials for several applications such as high performance composites[18-20],

7   components in water filters[21, 22], environmental sensors[23], building blocks for

8   electronic nanodevices[24], drug delivers[25] and others. What's more, graphene oxide

9   (GO), exhibiting high surface area and abundant surface functional group, has been

10   wildly studied for removing heavy metal ions[26]. However, with application of GO in

11   industry, biology and medicine, some people have reported that the GO can cause the

12   environmental pollution and bio-toxicology[27, 28] as well as the ILs, so besides

13   controlled the release of GO and ILs, we have to face a problem that the GO will be

14   excreted together with ILs into environment and water, and then the course of

15   pollution and detergents may be more complicated and hardly handled, so we must

16   make clear the relation between the GO and ILs in water. Although some researchers

17   have considered this problem and Alfonso S. Pensado *et al.* [29] reported the theory

18   study of interactions and structure of ionic liquids on graphene surfaces, there are no

19   experiment studies and it is unclear that the surface oxygen group affects the

20   interactions. Meanwhile Xing *et al.* [30, 31] showed the importance of π-π bonds and

21   carboxylic and lactonic group of carbon nanotubes on adsorption, and J Rivera-Utrilla

22   *et al.* [32]reported that π-cation interaction involves in carbon material adsorption

1 behaviors. Thereby, the level of oxygen of GO is an important factor to decide the

2 adsorption behavior on ILs, the common preparation method of rich oxygen GOs is to

3 control oxidation time of graphite, but this usually damage the structure of graphene

4 oxide and produced many carbonaceous fragments[33], which would affect adsorption

5 behavior of GO, meanwhile this method is harder and time-consuming. So we try to

6 prepare the GOs of different oxygen content *via* electron beam irradiation and

7 chemical reduction.

8 Most ILs are based on ammonium, phosphonium, imidazolium, pyridinium

9 cations[34], while the dialkylimidazolium salts have received much attention because of

10 their ease of synthesis and use in Friedel-Crafts reactions[35].

11 1-Butyl-3-methylimidazolium chloride ([bmim][Cl]) is a commercially available

12 dialkylimidazolium salt and other ionic liquids that should have similar surface

13 adsorption behaviors to [bmim][Cl] are ones with the same organic cation group, i.e.,

14 [bmim][PF6] and [bmim][BF4][36]. And we select 1-Butyl-3-methylimidazolium

15 chloride ([bmim][Cl]), 1-Butylpyridinium Chloride ([n-bPy][Cl]) and

16 1-butylimidazole with different properties as adsorbates for making clear the

17 adsorption mechanism of ionic liquids on graphene of different oxygen content.

18 **Experiment**

19 **Preparation materials**

20 Common graphene oxide (CGO) was prepared by an improved Hummers

21 method with graphite[37]. A 9:1 mixture of concentrated H_2SO_4/H_3PO_4 (360/40 mL) was

22 added to a mixture of graphite flakes (3.0 g) and $KMnO_4$ (18.0 g), producing a slight

1 exotherm to 35-40 °C. The reaction was then heated to 50 °C and stirred for 12 h. The

2 reaction was cooled to room temperature and poured onto ice (~400 mL) with 30%

3 H_2O_2 (3 mL). The solution was centrifuged (8000 rpm for 20min), and the supernatant

4 was decanted away. The remaining solid material was then washed and ultrasonicated

5 in succession with 200 mL of 30% HCl, then deionized water and ethanol，till pH~5.6.

6 The solid obtained was vacuum-dried overnight at 40 ^{o}C, obtaining 5.1 g of product.

7 The graphite were irradiated by electron beam of 600 MGy (Electron Accelerator

8 Center, Institute of Modern Physics, Chinese Academy of Sciences), then preparing

9 high oxygen content graphene oxide (HGO) by the improved Hummers method. The

10 CGO were reduced by HI at room temperature for 24h for obtaining graphene oxide

11 obtaining low oxygen content (LGO) [38].

12 **Characterization**

13 The prepared graphene oxide were collected and characterized by Transmission

14 electron microscopy (TEM), X-ray photoelectron spectroscopy (XPS), Raman spectra,

15 Fourier transform infrared (FTIR) spectra, BET and Potentiometric Titration. TEM

16 was examined using a Tecnai-G2-F30 Field Emission Transmission Electron

17 Microscope (FEI Corporation). Raman spectra from 500 to 4000 cm-1 were collected

18 on an inVia-Reflex Raman scope using a 632.8 nm He-Ne laser (Renishaw). FTIR

19 spectra were recorded from 400 to 4000 cm^{-1} on a NEXUS 670 5-DX 170SX

20 spectrometer (Nicolet Instrument Corporation). XPS spectra was examined using an

21 ESCALAB 250Xi (Thermo Fisher Scientific). Surface area was determined using a

22 multipoint Brunauer-Emmett-Teller (BET) method by ASAP 2020M. The

23 potentiometric acid–base titrations were conducted under argon using a DL50

24 Automatic Titrator (Mettler Toledo) in NaCl as background electrolyte.

25 **Adsorption Experiments**

1   Batch adsorption experiments were carried out at 250 rpm equivalent shaking

2   rate in a m/V=1 g/L adsorbent in 10 mL flasks containing 5 mL [bmim][Cl],

3   [n-bPy][Cl] (purchased from Institute of Lanzhou Chemistry Physics, Chinese

4   Academic of Science) and 1-Butylimidazole aqueous solution for 24 h. Initial ILs

5   concentrations from 0.05 to 1.5mmol/L were used. Adsorption kinetics experiments

6   demonstrated that 24 h was sufficient for reaching adsorption equilibrium. In most

7   experiments, solution pH was adjusted to 3-10 as measured with a pH-meter (pHS-3C,

8   Shanghai). For cases where pH was adjusted, a 0.1 mol/L NaOH or HCl solution was

9   used to change the initial pH value. A 5 mol/L NaCl background electrolyte solution

10   was used to adjust ionic strength. After each adsorption equilibrium, mixtures were

11   centrifuged, then [bmim][Cl], [n-bPy][Cl] and 1-butylimidazole concentration in the

12   supernatant were determined with a UV spectrophotometer(LAMBDA 35,

13   PerkinElmer) at 211, 258 and 208 nm. Adsorption amount was calculated according to

14   the difference of [bmim][Cl] concentrations before and after adsorption. In the

15   experiment of two ionic liquids interaction on adsorption behavior, one IL

16   concentration was fixed at 0.226 mmol/L, the other IL concentration was changed

17   from 0.05 to 1.5 mmol/L, and the adsorption amount of two ILs were measured and

18   calculated. At each condition, adsorption experiments were performed in triplicate and

19   average.

20   **Results and Discussion**

21   **Characterization results**

22   TEM images of three samples (*Fig. 1*) showed that the graphene oxide have been

1   successfully prepared. Raman spectra (*Fig. 2a*) of samples showed D peaks (1590

2   cm^{-1}) and G peaks (1350 cm^{-1}), confirming the lattice distortions, and the

3   enhancement of the I_D/I_G of LGO might be due to the decrease in the size of the newly

4   formed graphene like sp^2 domains[39, 40]. Also, FTIR spectra were recorded (*Fig. 2b*),

5   and the following functional groups were identified in all samples: O-H stretching

6   vibrations (3420 cm^{-1}), C=O stretching vibration (1727 cm^{-1}), C=C from unoxidized

7   sp^2 C-C bonds (1627 cm^{-1}), and C-O vibrations (1114 cm^{-1})[19].TEM images of LGO

8   (*Fig. 1b*) and HGO (*Fig. 1c*) showed that chemical reduction did not change the

9   structure of GO; but electron beam irradiation obviously defected structure of GO and

10 caused some fragments, which was attributed to damaging of electron beam

11 irradiation on precursor graphite (*Fig. 1d and e*). The C1s XPS spectra

12 (*Supplementary Information Fig. S1*) further confirmed this result, carbon sp^3

13 percentages of LGO, CGO and HGO were 32%, 53% and 57%, respectively. And

14 integrating peak of *C1s* and *O1s* XPS spectra, carbon to oxygen ratios of LGO, CGO

15 and HGO were 3.55, 2.26 and 1.85, respectively, which showed that the content of

16 surface oxygen groups increased gradually. The XPS results were similar to the report

17 of Cecilia Mattevi *et al.* [41] that perfect sp^2 structure of graphene increased with the

18 decrease of oxygen content after thermal treatment.

19   Potentiometric titrations[33, 42, 43] were performed under argon atmosphere to

20 characterize the surface charge densities (ΔQ^H, mol/g) of three samples. GO proton

21 excess which was equal to the surface charge density was determined by subtracting

22 the titration curve of the background electrolyte solution (blank) from that of GO

1   suspension. In general, a suspension of 0.5 g GO in 50 mL NaCl solution (0.01, 0.1,

2   0.4mol/L) was titrated with a standard NaOH solution (0.05 mol/L) up to pH~10 at

3   room temperature. The results (***Fig. 3***) showed that pH_{PZC} (pH of point of zero charge)

4   depended strongly on surface oxygen content and negatively on the ionic strength.

5    $$(C_A - C_B)_{susp} = [H^+] - [OH^-] + \Delta Q_{solid} + \Delta Q_{blank}$$

6    $$(C_A - C_B)_{blank} = [H^+] - [OH^-] + \Delta Q_{blank}$$

7    $$\Delta Q^H = V/m[(C_A - C_B)_{susp} - (C_A - C_B)_{blank}]$$

8   where C_A and C_B (mol/L) were the concentrations of acid and base added,

9   respectively; ΔQ_{blank} (mol/L) represented consumption or release of H^+ by side

10   reactions; ΔQ_{solid} (mol/L) and ΔQ^H (mol/g) represented the proton excess of the

11   graphene in different units, respectively; V (L) was the volume of aqueous solution

12   and m (g) was the mass of GO.

13   These results indicated that GO containing different oxygen content were

14   successfully prepared by electron beam irradiation and chemical reduction (detailed

15   data were summarized in ***Table 1***).

16   **Effect of graphene properties on adsorption**

17   The pH adsorption edges (***Fig. 4a***) and isotherms (***Fig. 4b***) of [bmim][Cl],

18   [n-bPy][Cl] and 1-Butylimidazole on LGO, CGO and HGO indicated that LGO

19   exhibited the highest adsorptive capacity, while CGO and HGO owned similar

20   adsorptive capacity, which was analogous to conclusion of Faria *et al.* [44] that though

21   acid oxygen-containing surface groups had a positive effect on the adsorption of dye

22   on activated carbon containing lower oxygen presented better performances. And with

1 the increase of surface oxygen content, the GOs became hydrophilic[45] and the

2 adsorption of ILs containing a hydrophobic alkyl chain would decrease. Machida *et al*.

3 [46] reported that graphene oxide had graphene layer sites and carboxylic and lactonic

4 groups sites (surface oxygen group**s** sites), as can be known from our characterization,

5 most of sites were graphene layer sites on LGO, both graphene layer sites and surface

6 oxygen groups sites distributed mainly on CGO, and HGO mainly contained surface

7 oxygen groups sites. Adsorption results convinced graphene layer sites performed

8 stronger adsorptive capacity of ILs than the surface oxygen group sites because of

9 best performance of LGO. The adsorption pH edges showed that adsorption peak of

10 LGO, CGO and HGO were 6, 6.4 and 8, generally moving to high pH side, as can be

11 known from view of Faria, different surface chemistries could change the *pHpzc* of

12 materials, and then affecting the adsorption of anionic and cationic dyes on activated

13 carbons, which fitted with change trend of pH_{PZC} for LGO (3.4), CGO (3.6) and HGO

14 (3.8) at ionic strength 0.01 mol/L (***Table 1***). Adsorption isotherms showed that the

15 adsorption quantities of ILs were lower than their respective monolayer coverage

16 within the tested concentrations (the surface coverages of the adsorbates on three

17 graphene samples were calculated by dividing the adsorbed amount with monolayer

18 adsorption capacity, ***Table 2***).

19 **Effect of ionic liquids properties on adsorption**

20 [a] data from http://ilthermo.boulder.nist.gov/index.html. [b] data from ref [47]. [c] data

21 from CRC Hand book of chemistry and physics 2010. [d] data HOMA (Harmonic

22 oscillator measure of aromaticity) was calculated according to ref [48, 49]. [e] data was

1   protonated 1-Butylimidazole. Q_m is the monolayer adsorption capacity (mmol/g)

2   calculated by $A_{surf}/(A_m \times N) \times 10^7$, where A_{surf} is the graphene surface area (m^2/g); A_m is

3   the projecting area of a single adsorbate molecule (cm^2) estimated by

4    $\pi \times (3MW/(4\pi \times D \times N))^{2/3}$, where N is the Avogadro constant, and MW is the molecular

5   weight (g/mol). K_F (mol^{n-1}L^n/g) and n is the Freundlich model coefficients obtained

6   from adsorption isotherm fitting results; R_F^2 is the correlation coefficient of the

7   Freundlich model. Q_∞(mmol/g) and $k(L/mol)$ are the Langmuir model coefficients

8   obtained from adsorption isotherm fitting results; R_L^2 is the correlation coefficient of

9   the Langmuir model.

10   **Aromaticity property of ILs on adsorption**

11   Electron Localization Function (ELF) was used to compare the aromaticity of

12   ILs. Density function of theory (DFT) was used to optimize the geometry of

13   adsorbents for getting their wavefunction. Then wavefunction was analyzed by

14   Multiwfn[50], images of ELF for adsorbents (***Fig. 5***) were drawn. After topology

15   analysis, bifurcation points and their isosurfaces (***Fig. 6***) were obtained. The results

16   suggested the aromaticity of [n-bPy]$^+$ was stronger than that of [bmim]$^+$, meanwhile,

17   [bmim]$^+$, 1-Butylimidazole and protonated 1-Butylimidazole were similar.

18   The pH adsorption edges (***Fig. 7a***) and isotherms (***Fig. 7b***) revealed that

19   [n-bPy][Cl] had higher absorbability than [bmim][Cl] on LGO with graphene layer

20   sites, which supported report of Xing[30] that aromaticity of organic could increase

21   organic compound adsorption on carbon nanotubes. On the contrary, the adsorption

22   percentage of [n-bPy][Cl] were much lower than that of [bmim][Cl] on surface

1   oxygen groups sites of HGO. This difference might be attributed to the structure

2   difference between [bmim][Cl] and [n-bPy][Cl], the extra nitrogen atom on

3   [bmim][Cl] had strong interaction with surface oxygen groups on graphene oxide,

4   such as the form of hydrogen bond. The potentiometric titrations results showed that

5   the ΔQ^H of three samples slowly decreased at low pH, and the ΔQ^H of CGO decreased

6   obviously at pH=7~8 which indicated the rapid deprotonation of CGO, resulting in

7   the hydrogen of CGO quickly decreased. So the interaction between the extra nitrogen

8   atom and surface oxygen groups on CGO is poor in accord with the change of

9   adsorptive ability of [bmim][Cl] and [n-bPy][Cl] on GO in the pH adsorption edges

10   (**Fig. 7a**). Adsorption isotherms of [bmim][Cl] and [n-bPy][Cl] on CGO (**Fig. 7c**)

11   under different pH could also confirm further the results.

12   **Cation property of ILs on adsorption**

13   J Rivera-Utrilla et al. [32] thought that cation interactions played an important role

14   on carbon material adsorption, and Zhu et al. [51] reported the polarity property of

15   organic chemical affected the adsorption on carbon nanotubes. So the adsorption of

16   [bmim][Cl] and its organic analogue 1-Butylimidazole was studied to understand the

17   effect of cation property. The pH adsorption edges of [bmim][Cl] and

18   1-Butylimidazole on LGO, CGO and HGO (**Fig. 8**) showed that the adsorption

19   behaviors of two compound were similar in acid solution; but adsorbability of

20   [bmim][Cl] was stronger than that of 1-Butylimidazole in alkaline solution.

21   In acid solution (pH<*pKa*), 1-Butylimidazole was protonated by H^+ and like an

22   cation, and [bmim]$^+$ and protonated 1-Butylimidazole were similar in aromaticity,

1   thus the adsorption behavior of 1-Butylimidazole would be similar to that of

2   [bmim][Cl].

3   However in alkaline solution (pH>pK_a), 1-Butylimidazole would be present as

4   molecular, suggesting that π-cation or electrostatic interaction between

5   1-Butylimidazole and graphene oxide was not formed, so the adsorption of

6   1-Butylimidazole on graphene oxide was lower than that of $[bmim]^+$. In detailed, the

7   adsorption percentage of [bmim][Cl] and 1-Butylimidazole on HGO was higher than

8   that of CGO and LGO, it might be result from that the surface oxygen group on HGO

9   were much more than that of CGO and LGO, Thomas *et al.* [52] reported that cation

10   exchange and adsorption capacity decreased significantly after heat treatment of the

11   oxidized carbons to remove oxygen functional groups. The results indicated that there

12   was interaction between the surface oxygen group and the cation property of GO,

13   such as electrostatic attraction and ion exchange.

14   **Effect of ionic strength on adsorption**

15   The pH adsorption edges of [bmim][Cl] and [n-bPy][Cl] on CGO in different

16   ionic strength (*Fig. 9a*) showed that the adsorption percentage obviously decreased

17   with the increase of ionic strength. And the peak of pH adsorption edges of bmim][Cl]

18   on CGO were respectively 6.5, 5.5 and 5 at ionic strength 0.01, 0.1 and 1mol/L NaCl,

19   and gradually moved to low pH side, the results could also be explained by Faria's

20   conclusion.

21   The effect of NaCl concentration to the adsorption of ionic liquid (*Fig. 10*)

22   showed that the adsorption percentages decreased on LGO and CGO and increased on

1 HGO with the increase of NaCl concentration. Goldberg *et al.* [53] reported chemical

2 bonds between adsorbent and adsorbate could form inner-sphere surface complexes,

3 leading to tiny change of the adsorption percentage with the increase of ionic strength;

4 while non-chemical bond between adsorbent and adsorbate could form outer-sphere

5 surface complexes, leading to that the adsorption percentage decreased with the

6 increase of ionic strength. XPS and potentiometric titration results showed that the

7 great amount of surface oxygen group on HGO mainly existed as molecular form at

8 pH=4 (closed to pH_{PZC}), which formed hydrogen bond and coordination (both

9 chemical bond) with ILs, so the adsorption on HGO changed slightly with the

10 increase of NaCl concentration; but LGO containing little surface oxygen group

11 mainly formed π-π and π-cation[54] interaction (both nonchemical bond) with ILs, so

12 the adsorption decreased obviously on LGO with the increase of NaCl concentration;

13 and both chemical and nonchemical bond existed on CGO, so the adsorption

14 decreased gradually on CGO with the increase of NaCl concentration.

15 **Two ionic liquids interaction on adsorption**

16 As can be seen from the interaction between ILs on LGO, CGO and HGO (***Fig.***

17 ***11***), the adsorption of two ILs were reciprocal inhibition on LGO; but for that on CGO

18 and HGO, one IL could promote the adsorption of another IL. It was obvious that the

19 adsorption of two ILs on GO interplayed. And the difference could be attributed to

20 surface chemistries of LGO, CGO and HGO and the properties of ILs.

21 There were mainly graphene layer sites on LGO and few surface oxygen groups

22 sites, so the surface oxygen group sites having weak adsorption capacity could be

1 negligible. So the competitive adsorption between [bmim][Cl] and [n-bPy][Cl] was

2 observed in *Fig.11a-b*, the adsorption of [n-bPy][Cl] with stronger aromaticity was

3 stronger than that of [bmim][Cl] on LGO.

4 Both of graphene layer sites and surface oxygen groups sites were abundant on

5 CGO. The adsorption of [n-bPy][Cl] increased with the increase of concentration

6 (*Fig.11c*), and [n-bPy][Cl] with strong adorability occupied mainly graphene layer

7 sites, so the adsorption of [bmim][Cl] was decreased. However, the [bmim][Cl] owns

8 an electron-rich aromatic ring[55], so adsorption of [bmim][Cl] improved electron

9 density on CGO and promoted the adsorption of [n-bPy][Cl] which had an

10 electron-deficient group[56], which caused the increase of the adsorption of [n-bPy][Cl]

11 compared to that it existed alone. As can be seen from *Fig.11d*, the adsorption of

12 [bmim][Cl] depended on concentration, which occurred mainly on the surface oxygen

13 group sites. And the adsorption of [bmim][Cl] carrying electron-rich aromatic ring

14 could increase the adsorption of [n-bPy][Cl] carrying electron-deficient aromatic ring

15 on graphene layer sites, so the adsorption of [n-bPy][Cl] increased slightly, but

16 adsorption of [bmim][Cl] was poorer than that of single in absence of [n-bPy][Cl],

17 because [n-bPy][Cl] occupied the graphene layer sites with strong absorbability.

18 Surface oxygen group sites were main adsorption sites on HGO, but the

19 graphene layer sites could not be ignored because it owned strong absorbability of ILs.

20 The adsorption of [n-bPy][Cl] on HGO increased with the increase of concentration

21 (*Fig.11e*), the adsorption of electron-deficient [n-bPy][Cl] increased the adsorption of

22 electron-rich [bmim][Cl] on surface oxygen group sites, so the adsorption of

1 [bmim][Cl] increased somewhat; the adsorption of [n-bPy][Cl] on surface oxygen

2 group sites was lower than that of single in absence of [bmim][Cl], so the adsorption

3 of [n-bPy][Cl] on HGO decreased compared with single adsorption. In *Fig.11f*, the

4 adsorption of [bmim][Cl] increased with the increase of concentration, which promote

5 the adsorption of electron-deficient [n-bPy][Cl] on graphene layer sites, but hardly

6 offset the negative adsorption on surface oxygen group sites, so the adsorption of

7 [n-bPy][Cl] decreased. However, the adsorption of electron-deficient [n-bPy][Cl] on

8 graphene layer sites of HGO could promote the adsorption of [bmim][Cl] on surface

9 oxygen group sites obviously and the promotion gradually decreased with decrease of

10 adsorption of [n-bPy][Cl].

11 **Conclusion**

12 Electron beam irradiation successfully increased the surface oxygen content and

13 partially changed the layer structure of graphene, while chemical reduction decreased

14 the surface oxygen content. Because of graphene layer sites forming nonchemical

15 bond and surface oxygen group sites forming chemical bond with ILs, graphene layer

16 sites were proved to be stronger than surface oxygen group sites on absorbability at

17 low ionic strength, while surface oxygen group sites were proved to be stronger than

18 graphene layer sites on absorbability at high ionic strength. Aromaticity and cation

19 properties of ILs would promote the adsorption of ILs on GO. The adsorption of

20 [n-bPy][Cl] on graphene layer sites was stronger than that of [bmim][Cl], on the

21 contrary, the adsorption of [bmim][Cl] is stronger than that of [n-bPy][Cl] on

22 surface oxygen group sites. Through investigating interaction between ILs on

adsorption, the adsorption of two ILs was reciprocal inhibition on LGO containing

low oxygen content; but for that on CGO and HGO containing high oxygen content,

one IL could promote the adsorption of another IL.

Acknowledgments

References

1. K. M. Docherty andC. F. Kulpa Jr, *Green Chemistry*, **2005,** *7*, 185-189.

2. H. Li,P. S. Bhadury,B. Song andS. Yang, *RSC Advances*, **2012,** *2*, 12525-12551.

3. J. F. Wishart, *Energy & Environmental Science*, **2009,** *2*, 956-961.

4. N. D. Khupse andA. Kumar, *Indian journal of chemistry. Section A, Inorganic, bio-inorganic, physical, theoretical & analytical chemistry*, **2010,** *49*, 635.

5. S. Murugesan andR. J. Linhardt, *Current organic synthesis*, **2005,** *2*, 437-451.

6. T. Nonthanasin,A. Henni andC. Saiwan, *RSC Advances*, **2014,** *4*, 7566-7578.

7. Y. Luo,Q. Wang,Q. Lu,Q. Mu andD. Mao, *Environmental Science & Technology Letters*, **2014**.

8. V. Jaitely,A. Karatas andA. T. Florence, *International journal of pharmaceutics*, **2008,** *354*, 168-173.

9. S.-M. Lee,W.-J. Chang,A.-R. Choi andY.-M. Koo, *Korean Journal of Chemical Engineering*, **2005,** *22*, 687-690.

10. A. Yokozeki andM. B. Shiflett, *Industrial & Engineering Chemistry Research*, **2010,** *49*, 9496-9503.

11. J. Nichthauser,W. Mrozik,A. Markowska andP. Stepnowski, *Chemosphere*, **2009,** *74*, 515-521.

12. C. K. Chua andM. Pumera, *Chemical Society Reviews*, **2013,** *42*, 3222-3233.

13. J. Park andM. Yan, *Accounts of chemical research*, **2012,** *46*, 181-189.

14. V. Singh,D. Joung,L. Zhai,S. Das,S. I. Khondaker andS. Seal, *Progress in Materials Science*, **2011,** *56*, 1178-1271.

15. Y. Zhu,S. Murali,W. Cai,X. Li,J. W. Suk,J. R. Potts andR. S. Ruoff, *Advanced materials*, **2010,** *22*, 3906-3924.

16. W. Qi,J. Bi,X. Zhang,J. Wang,J. Wang,P. Liu,Z. Li andW. Wu, *Scientific reports*, **2014,** *4*.

17. Q. Wei,L. Zhan,B. Juanjuan,W. Jing,W. Jianjun,S. Taoli,G. Yi'an andW. Wangsuo, *Nanoscale research letters*, **2012,** *7*, 1-9.

18. L. Wang,Y. Huang,X. Ding,P. Liu andM. Zong, *RSC Advances*, **2013,** *3*, 23290-23295.

19. Y. Hu,J. Shen,N. Li,M. Shi,H. Ma,B. Yan,W. Wang,W. Huang andM. Ye, *Polymer Composites*, **2010,** *31*, 1987-1994.

20. X. An andJ. C. Yu, *RSC Advances*, **2011,** *1*, 1426-1434.

21. M. A. Shannon,P. W. Bohn,M. Elimelech,J. G. Georgiadis,B. J. Mariñas andA. M. Mayes, *Nature*, **2008,** *452*, 301-310.

22. D. Cohen-Tanugi andJ. C. Grossman, *Nano letters*, **2012,** *12*, 3602-3608.

23. M. Pumera,A. Ambrosi,A. Bonanni,E. L. K. Chng andH. L. Poh, *TrAC Trends in Analytical Chemistry*, **2010,** *29*, 954-965.

24. Y.-M. Lin andP. Avouris, *Nano letters*, **2008,** *8*, 2119-2125.

25. X. Sun,Z. Liu,K. Welsher,J. T. Robinson,A. Goodwin,S. Zaric andH. Dai, *Nano research*, **2008,** *1*, 203-212.

26. Y. Sun,Q. Wang,C. Chen,X. Tan andX. Wang, *Environmental science & technology*, **2012,** *46*, 6020-6027.

27. K. Yang,J. Wan,S. Zhang,Y. Zhang,S.-T. Lee andZ. Liu, *ACS nano*, **2010,** *5*, 516-522.

28. L. Zhan,G. Yanxia,Z. Xiaoyong,Q. Wei,F. Qiaohui,L. Yan,J. Zongxian,W. Jianjun,T. Yuqin andD. Xiaojiang, *Journal of Nanoparticle Research*, **2011,** *13*, 2939-2947.

29. A. S. Pensado,F. Malberg,M. F. C. Gomes,A. A. H. Padua,J. Fernandez andB. Kirchner, *RSC Advances*, **2014,** *4*, 18017-18024.

30. B. Pan andB. Xing, *Environmental Science & Technology*, **2008,** *42*, 9005-9013.

31. D. Lin andB. Xing, *Environmental science & technology*, **2008,** *42*, 7254-7259.

32. J. Rivera-Utrilla andM. Sanchez-Polo, *Water Research*, **2003,** *37*, 3335-3340.

33. Z. Guo,S. Wang,G. Wang,Z. Niu,J. Yang andW. Wu, *Carbon*, **2014**.

34. S. Keskin,D. Kayrak-Talay,U. Akman andÖ. Hortaçsu, *The Journal of Supercritical Fluids*, **2007,** *43*, 150-180.

35. M. J. Earle andK. R. Seddon, *Pure and applied chemistry*, **2000,** *72*, 1391-1398.

36. D. J. Gorman-Lewis andJ. B. Fein, *Environmental science & technology*, **2004,** *38*, 2491-2495.

37. D. C. Marcano,D. V. Kosynkin,J. M. Berlin,A. Sinitskii,Z. Sun,A. Slesarev,L. B. Alemany,W. Lu andJ. M. Tour, *ACS nano*, **2010,** *4*, 4806-4814.

38. S. Pei,J. Zhao,J. Du,W. Ren andH.-M. Cheng, *Carbon*, **2010,** *48*, 4466-4474.

39. S. H. Aboutalebi,A. T. Chidembo,M. Salari,K. Konstantinov,D. Wexler,H. K. Liu andS. X. Dou, *Energy & Environmental Science*, **2011,** *4*, 1855-1865.

40. W. Gao,L. B. Alemany,L. Ci andP. M. Ajayan, *Nature Chemistry*, **2009,** *1*, 403-408.

41. C. Mattevi,G. Eda,S. Agnoli,S. Miller,K. A. Mkhoyan,O. Celik,D. Mastrogiovanni,G. Granozzi,E. Garfunkel andM. Chhowalla, *Advanced Functional Materials*, **2009,** *19*, 2577-2583.

42. P. J. Swedlund,J. G. Webster andG. M. Miskelly, *Geochimica et Cosmochimica Acta*, **2009,** *73*, 1548-1562.

43. Z. Guo,J. Xu,K. Shi,Y. Tang,W. Wu andZ. Tao, *Colloids and Surfaces A: Physicochemical and Engineering Aspects*, **2009,** *339*, 126-133.

44. P. Faria,J. Orfao andM. Pereira, *Water Research*, **2004,** *38*, 2043-2052.

45. S. Stankovich,D. A. Dikin,R. D. Piner,K. A. Kohlhaas,A. Kleinhammes,Y. Jia,Y. Wu,S. T. Nguyen andR. S. Ruoff, *Carbon*, **2007,** *45*, 1558-1565.

46. M. Machida,T. Mochimaru andH. Tatsumoto, *Carbon*, **2006,** *44*, 2681-2688.

47. T. L. Amyes,S. T. Diver,J. P. Richard,F. M. Rivas andK. Toth, *Journal of the American Chemical Society*, **2004,** *126*, 4366-4374.

48. T. M. Krygowski, *Journal of chemical information and computer sciences*, **1993,** *33*, 70-78.

49. H. Fallah-Bagher-Shaidaei,C. S. Wannere,C. Corminboeuf,R. Puchta andP. v. R. Schleyer, *Organic*

1 *letters,* **2006,** *8*, 863-866.

2 50. T. Lu and F. Chen, *Journal of Computational Chemistry*, **2012,** *33*, 580-592.

3 51. W. Chen, L. Duan and D. Zhu, *Environmental Science & Technology*, **2007,** *41*, 8295-8300.

4 52. Y. Jia and K. Thomas, *Langmuir*, **2000,** *16*, 1114-1122.

5 53. S. Goldberg, *Journal of colloid and interface science*, **2005,** *285*, 509-517.

6 54. J. C. Ma and D. A. Dougherty, *Chemical reviews*, **1997,** *97*, 1303-1324.

7 55. C. Li, Q. Wang and Z. K. Zhao, *Green Chemistry*, **2008,** *10*, 177-182.

8 56. B. Dong, T. Sakurai, Y. Honsho, S. Seki and H. Maeda, *Journal of the American Chemical Society*, **2013,**

9 *135*, 1284-1287.

10

11

Figure and table

The Adsorption of Water-soluble Ionic Liquids on Graphene Oxide of Different Oxygen Content

Tian Longlong[1] and Zhang Xin[2], Qi Wei[1], Liu Dan[1], Jin Qiang[1], Lin Jing[1], Ye Yuanlv[4], Li Zhan[3*], Wu Wangsuo[1*]

1. Radiochemical Laboratory, Lanzhou University, Lanzhou, Gansu, China, 730000

2. Institute of Modern Physics, Chinese Academy of Sciences, Lanzhou, Gansu, China, 730000

3. Lanzhou Institute of Chemistry Physics, Chinese Academic of Science，Lanzhou, Gansu, China, 730000

4. Nuclear and Radiation Safety Center, Ministry of Environmental Protection of China, Beijing, China, 100082
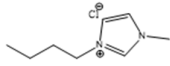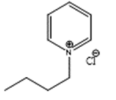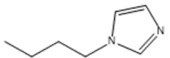
Corresponding author: Li Zhan, Email: lizhancg@licp.cas.cn; Wu Wangsuo, Email: wuws@lzu.edu.zn.

Table 1 Selected Properties of Three Graphene Oxide Samples

material	surface EC[a] (%)			C/O	I_D/I_G[c]	pH$_{PZC}$[d]			A$_{surf}$(m²/g)[e]
	C	C$_{sp3}$[b]	O			I=0.01mol/L	I=0.1mol/L	I=0.4mol/L	
LGO	78	32	22	3.55	1.68	3.4			261
CGO	69.35	53	30.65	2.26	1.47	3.6	3.2	2.7	229
HGO	64.92	57	35.08	1.85	1.57	3.8			256

[a] data surface elemental contents (EC) were measured by XPS. [b] data oxidized carbon(C$_{sp3}$) percentages were calculated by analyzing the C1s XPS spectra. [c] data I_D/I_G was calculated by integrating D peak and G peak. [d] data pH$_{PZC}$(pH of was measured by Potentiometric Titration. [e] data surface area (A$_{surf}$) was calculated from the adsorption-desorption isotherm of N$_2$ at 77 K by the multipoint BET method.

Table 2 Summary of Adsorbate Properties and Freundlich/Langmuir Model (S4) Coefficients Obtained from Adsorption Isotherms Fitting

| name	structure	D[a]	pk$_a$	HOMA[d]	material	Q$_m$	pH	K$_F$	n	R$_F^2$	Q$_\infty$	k	R$_L^2$
[bmim][Cl]		1.05	22[b]	0.767	CGO	0.708	2.5	0.013±0.007	0.752±0.079	0.921	0.351±0.053	262±189	0.895
							5.5	0.002±0.0007	0.563±0.043	0.934	0.083±0.01	1599±367	0.91
							10	71.548±45.749	2.098±0.099	0.991	0.139±0.002	484±102	0.988
					HGO	0.792	5.5	0.039±0.015	0.821±0.054	0.973	0.457±0.043	412±159	0.972
					LGO	0.807	5.5	0.454±0.118	1.061±0.037	0.978	1.25±0.05	294±49	0.949
[n-bPy][Cl]		-	-	0.967	CGO	-	2.5	0.003±0.002	0.596±0.071	0.918	0.09±0.012	1530±422	0.942
							5.5	0.142±0.110	1.095±0.110	0.953	0.293±0.024	295±121	0.961
							10	0.001±0.0002	0.390±0.029	0.958	0.074±0.01	5230±971	0.933
					HGO	-	5.5	0.058±0.005	0.929±0.012	0.998	0.694±0.012	144±22	0.999
					LGO	-	5.5	0.001±0.0003	0.319±0.032	0.949	0.152±0.029	8561±2219	0.889
1-Butylimidazole		0.945	7.75[c]	0.783 / 0.791[e]	CGO	0.829	5.5	0.0002±0.00006	0.196±0.036	0.898	0.043±0.004	47710±5357	0.993
					HGO	0.938	5.5	-0.029±0.006	0.855±0.032	0.989	0.361±0.014	288±52	0.137
					LGO	0.945	5.5	0.001±0.002	0.303±0.229	0.139	0.086±0.072	34564±41267	0.984
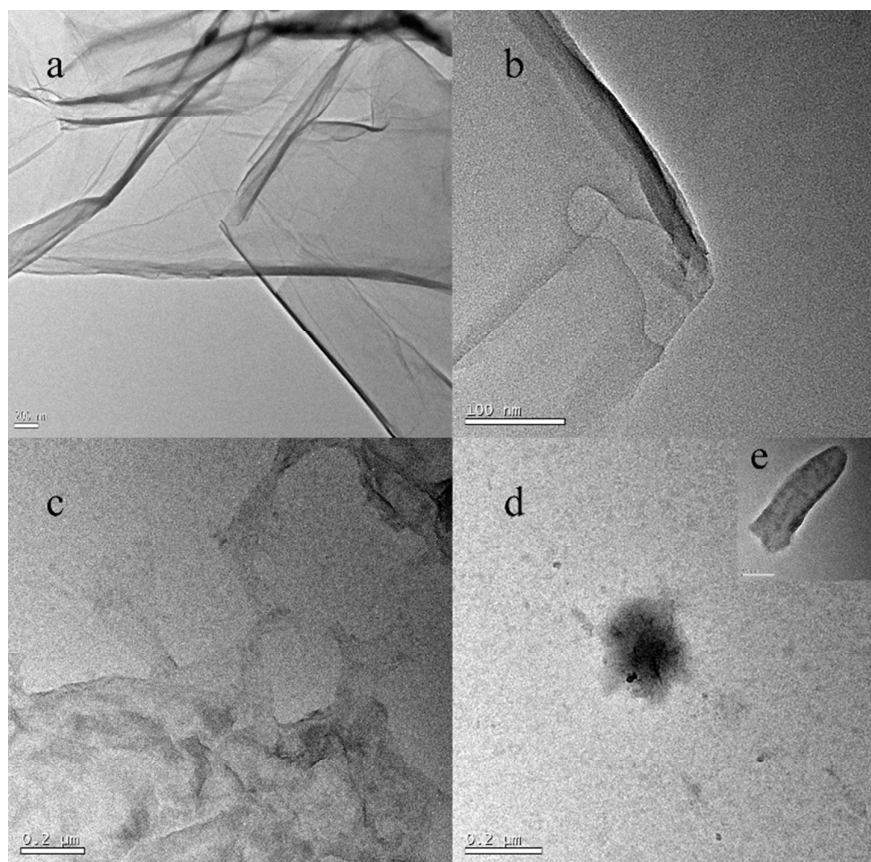
Figure 1 TEM images of CGO (a), LGO (b), HGO (c), and electron beam irradiated graphite (d) and initial graphite (e).
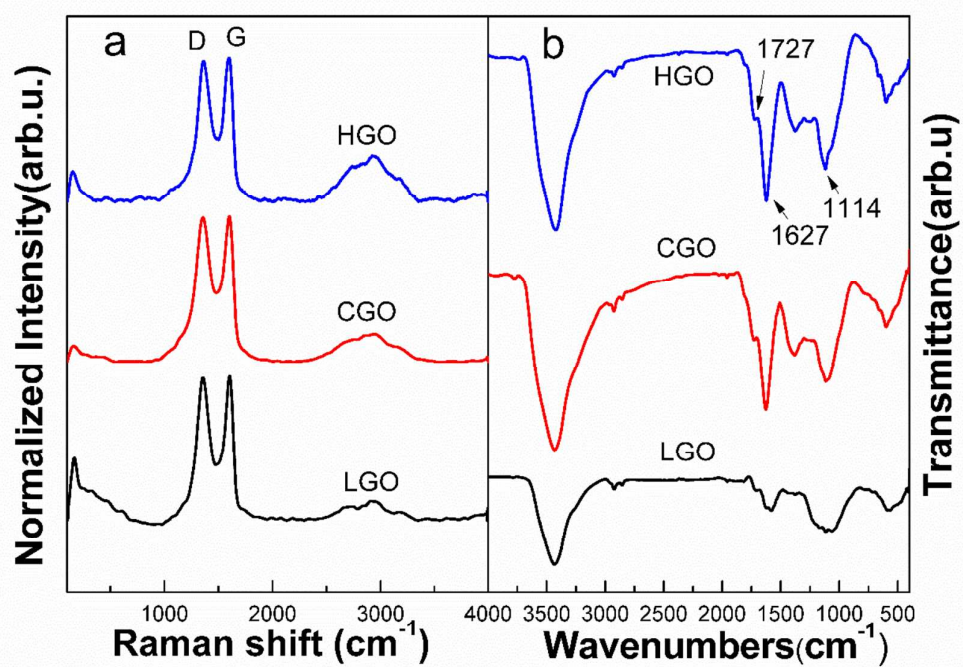
Figure 2 Raman (a) and FTIR (b) of LGO, CGO and HGO.
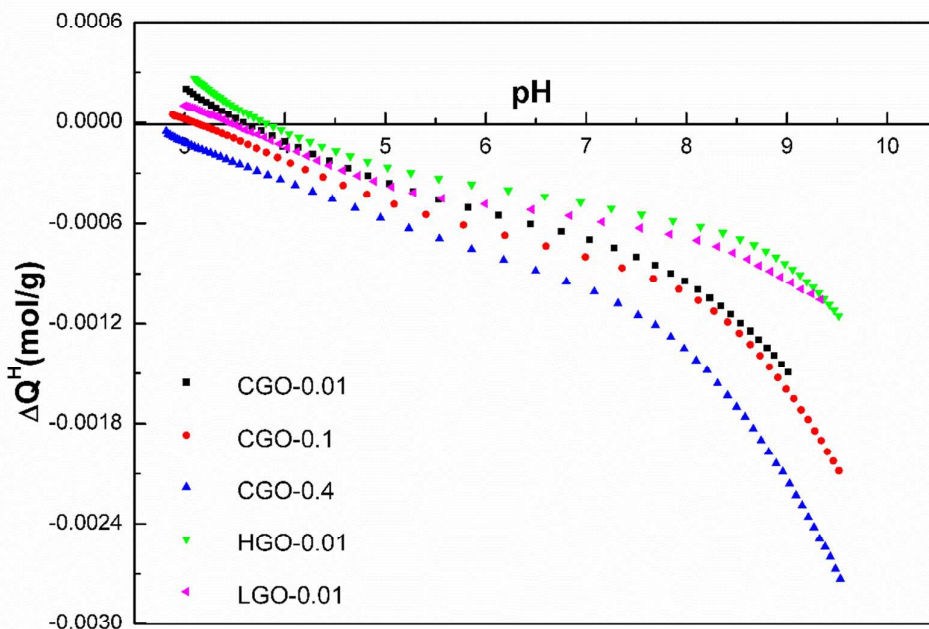
**Figure 3** surface charge density of graphene oxide at different ionic strength.
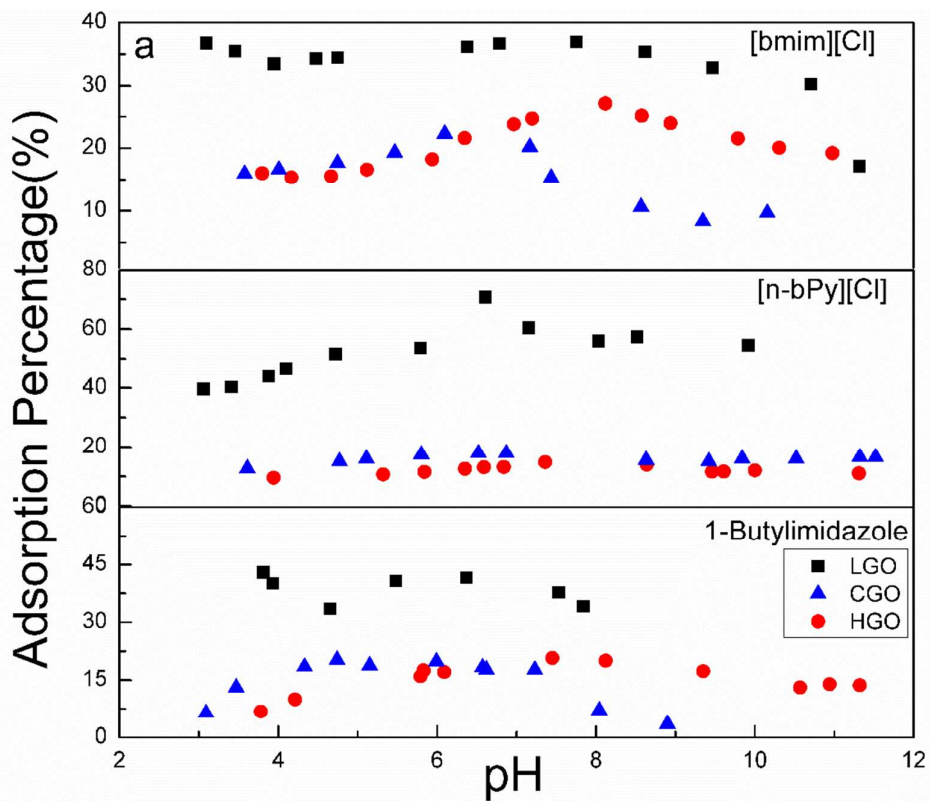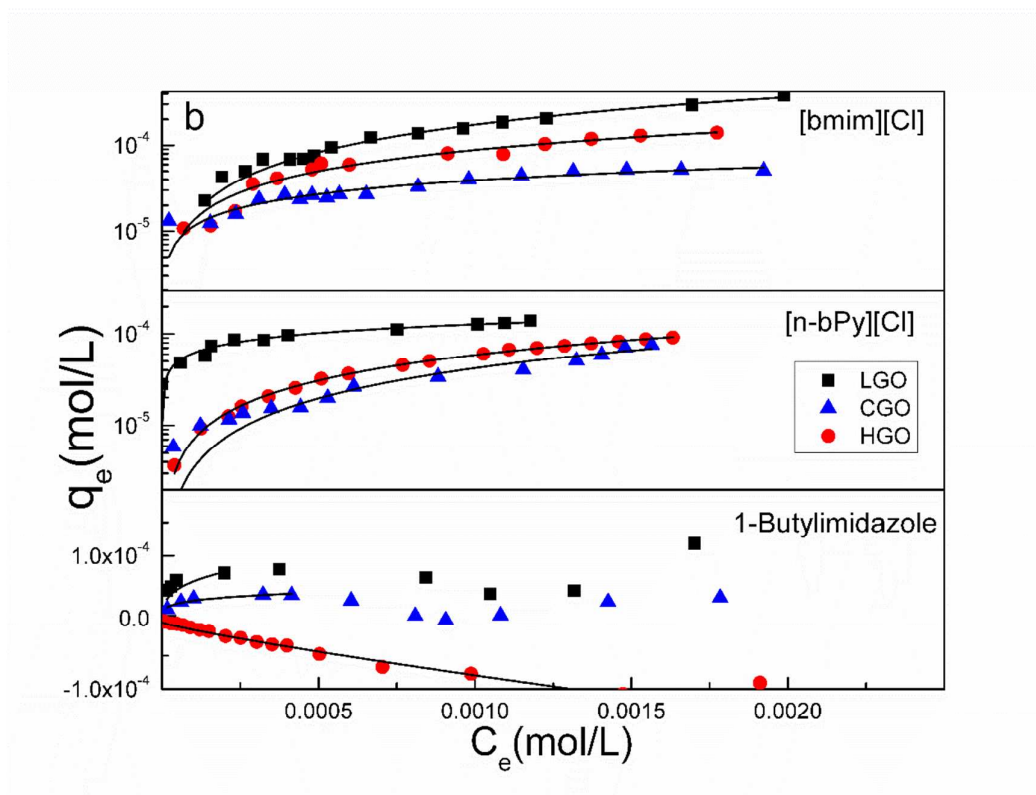
Figure 4 pH adsorption edges of [bmim][Cl], [n-bPy][Cl] and 1-Butylimidazole on LGO, CGO and HGO at ionic strength I=0.01 mol/L and initial concentration C_0=2.094×10^{-4} mol/L(a). Adsorption isotherm of [bmim][Cl], [n-bPy][Cl] and 1-butylimidazole on LGO, CGO and HGO at pH=5.5 and ionic strength I=0.1mol/L(b). The black lines were the Freundlich model fitting results.
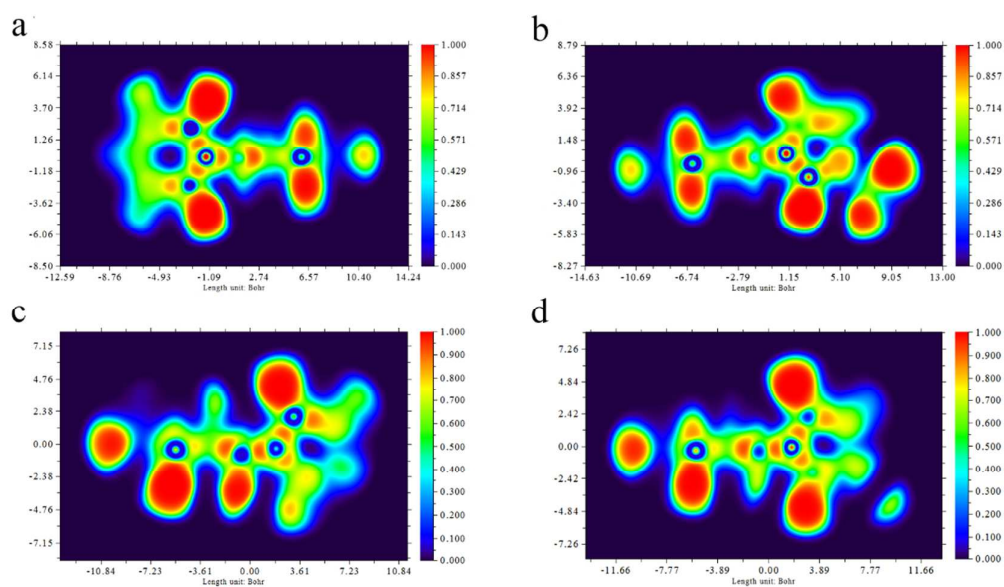
Figure 5 Electron Localization Functions-XY plane of [bmim]$^+$ (a), [n-bPy]$^+$ (b), 1-Butylimidazole(c) and protonated 1-Butylimidazole(d).
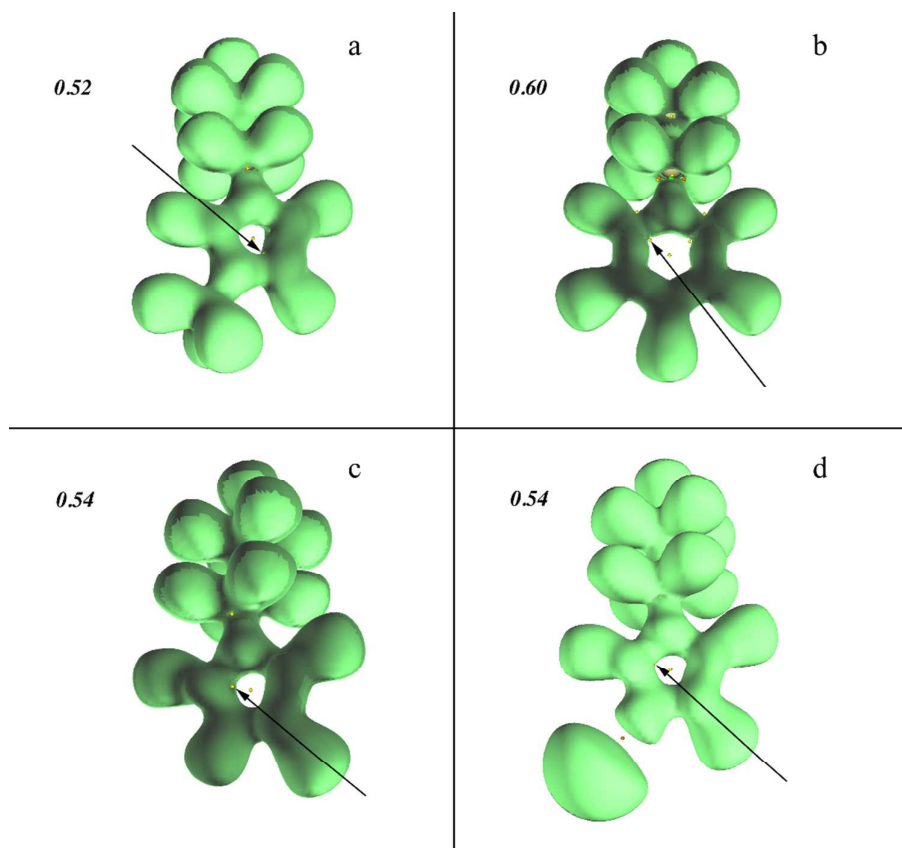
Figure 6 Bifurcation points (black arrow) and their isosurfaces of [bmim]$^+$ (a), [n-bPy]$^+$ (b), 1-Butylimidazole(c) and protonated 1-Butylimidazole(d).
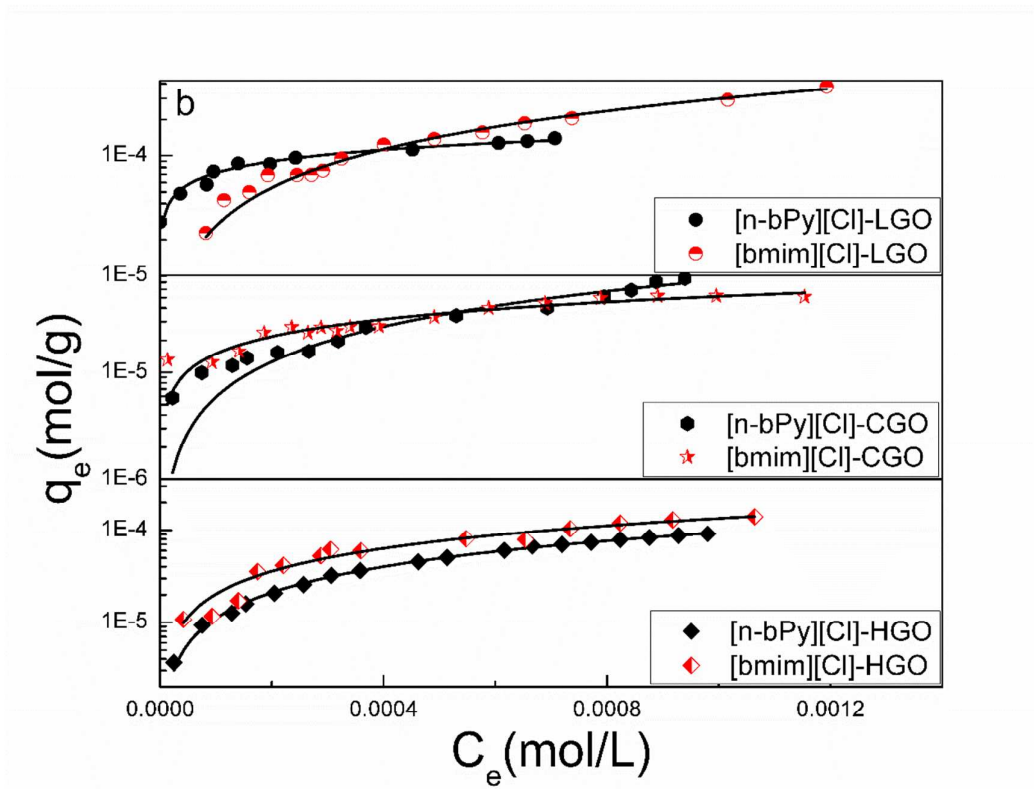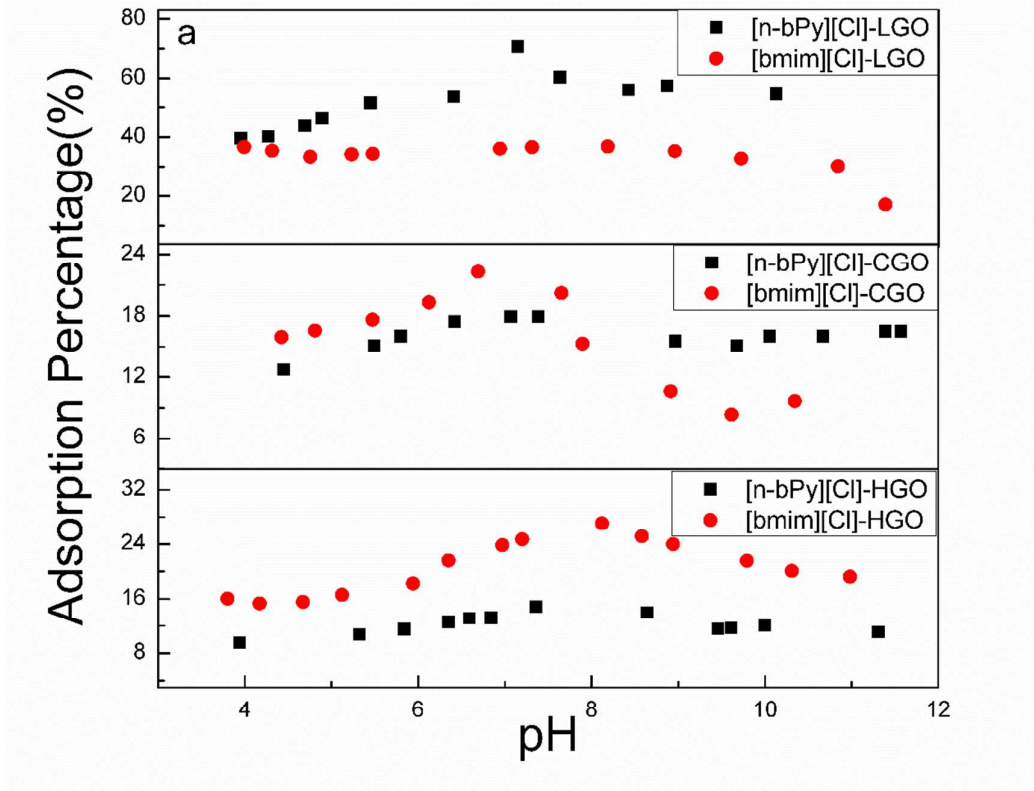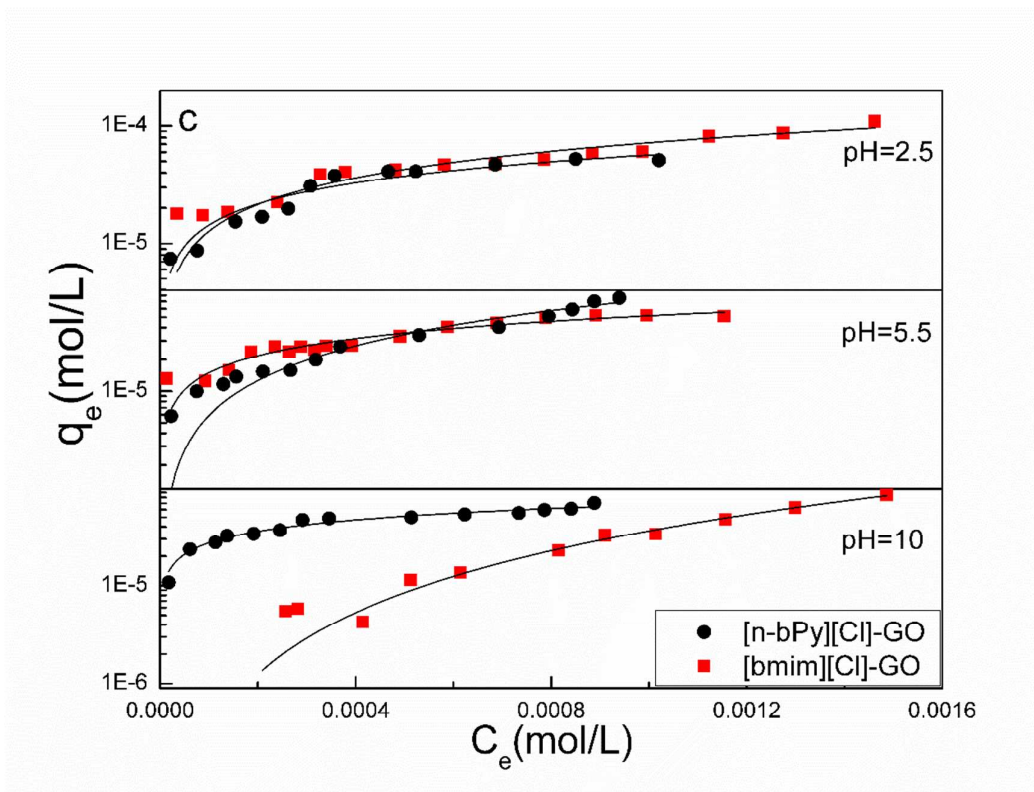
Figure 7 Comparing adsorption of [bmim][Cl] and [n-bPy][Cl] on LGO, CGO and HGO as a function of pH at ionic strength I = 0.01 mol/L and initial equal concentration $C_0=2.62\times10^{-4}$ mol/L(a). Adsorption isotherms of [bmim][Cl] and [n-bPy][Cl](f) at pH=5.5 and ionic strength I=0.1mol/L(b). Adsorption isotherms of [bmim][Cl] and [n-bPy][Cl] on CGO at different pH and ionic strength I=0.1mol/L(c). The black lines were the Freundlich model fitting results.
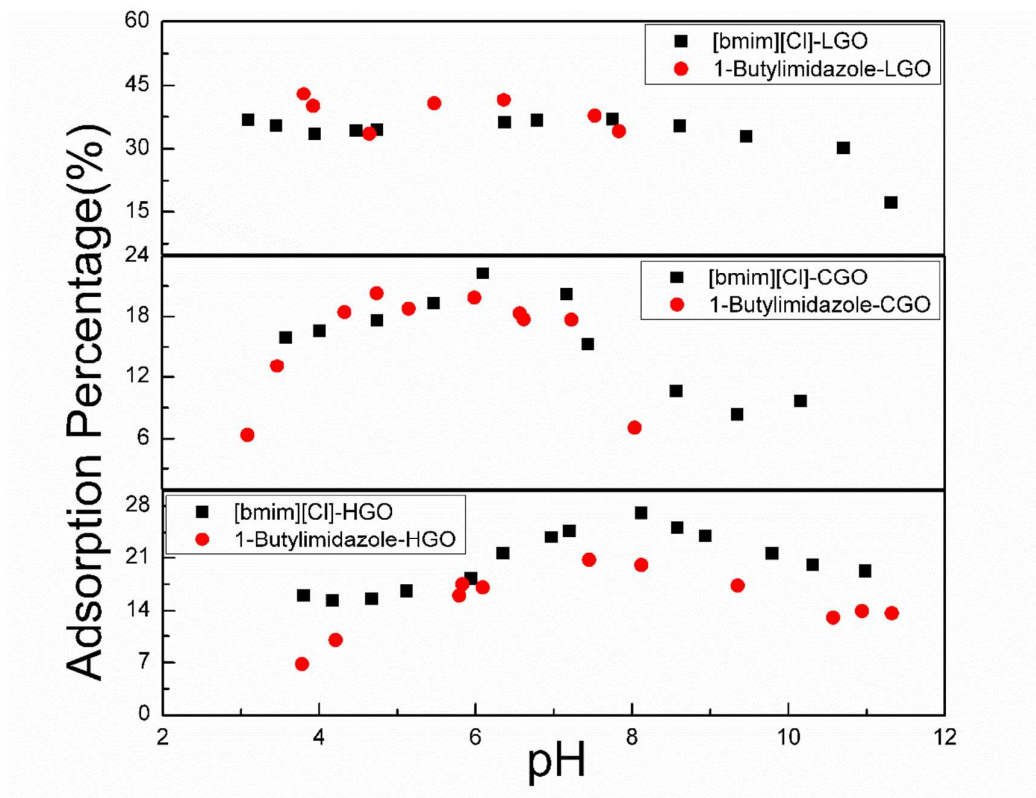
Figure 8 Comparing adsorption of [bmim][Cl] and 1-Butylimidazole on LGO, CGO and HGO as a function of pH at ionic strength I = 0.01 mol/L and initial equal concentration C_0=2.09×10^{-4} mol/L.
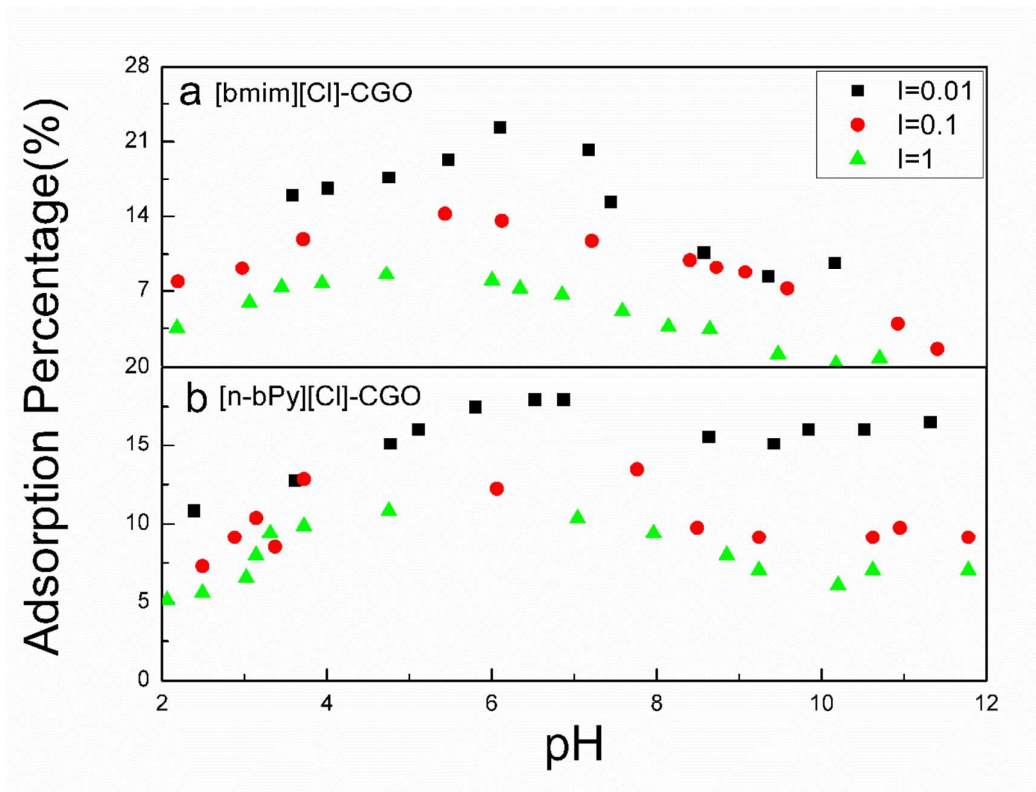
Figure 9 pH adsorption edge of [bmim][Cl]（a）and [n-bPy][Cl]（b）on CGO at different ionic strength, initial concentration $C_0=2.09\times10^{-4}$mol/L.
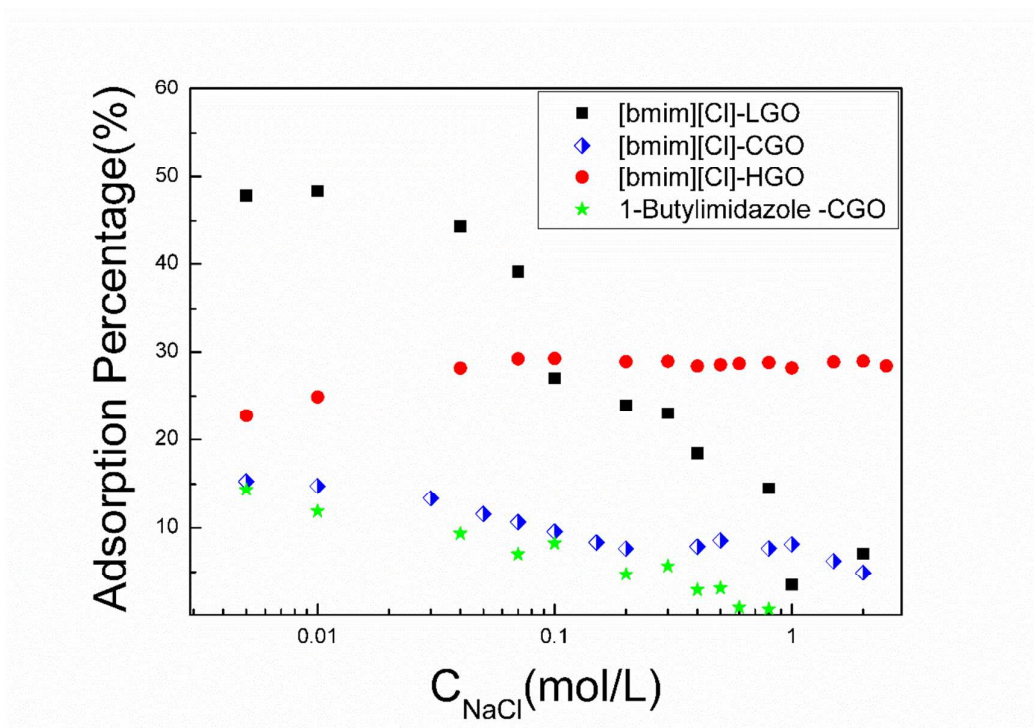
Figure 10 the effect of NaCl concentration to the adsorption of ionic liquid on graphene oxide at pH=4 and initial concentration of IL $C_0=2.09\times10^{-4}$mol/L.
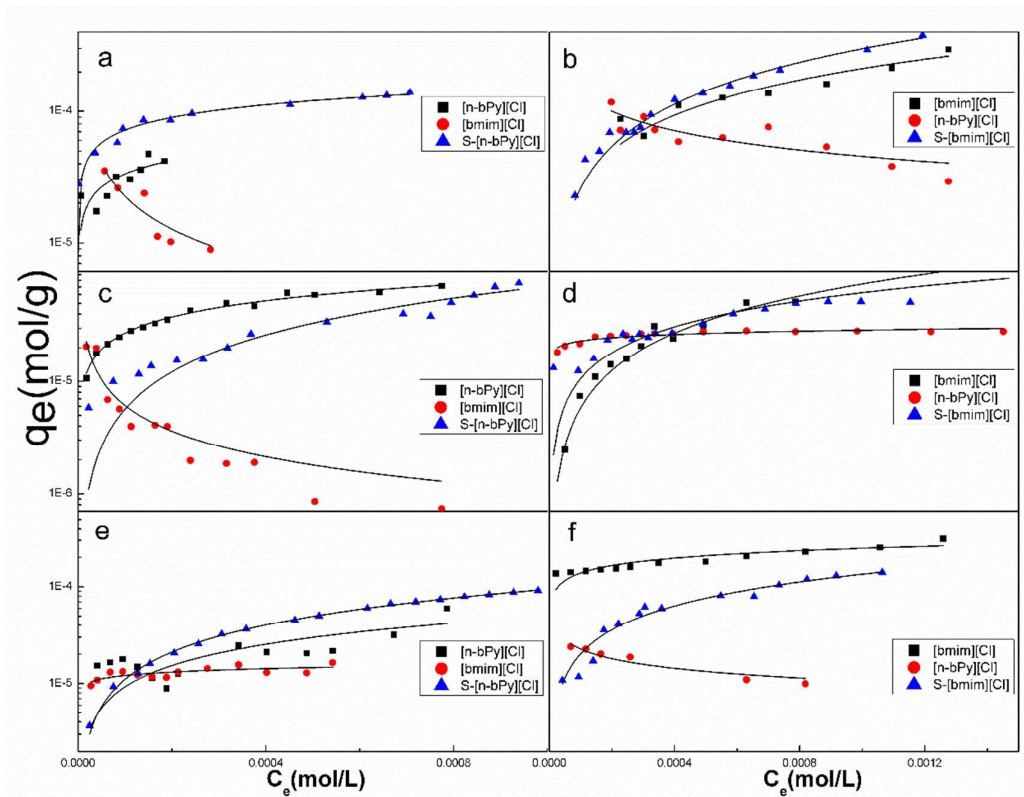
Figure 11 interaction between ILs on LGO (a, b), CGO (c, d) and HGO (e, f) at pH=4 and ionic strength 0.01mol/L, fixed ILs initial concentration C_0=2.62×10^{-4}mol/L. The black lines were the Freundlich model fitting results.